

# An Electrochemical-Thermal Multiphysics Model for Lithium Polymer Battery

Marcel Roy B. Domalanta<sup>a</sup>, Michael T. Castro<sup>a</sup>, Joey D. Ocon<sup>a,b</sup>, Julie Anne D. del Rosario<sup>a,\*</sup>

<sup>a</sup>Laboratory of Electrochemical Engineering (LEE), Department of Chemical Engineering, University of the Philippines Diliman, Quezon City 1101, Philippines

<sup>b</sup>Energy Engineering Program, National Graduate School of Engineering, College of Engineering, University of the Philippines Diliman, Quezon City 1101, Philippines  
 jddelrosario2@up.edu.ph

With the rising energy demand, safe and efficient energy storage technologies have been increasing in importance. Lithium Polymer (LiPo) batteries use a gel polymer to act as both separator and electrolyte, which is thermally and electrochemically more stable and safer than conventional liquid electrolytes. Besides exploring new materials, engineering a reliable multiphysics model is vital to exploiting and optimizing existing LiPo batteries' potential. This study developed a multiphysics model for a Lithium Cobalt Oxide (LCO)-graphite-Poly(vinylidene fluoride - hexafluoropropylene) (PVdF-HFP) pouch-type mobile phone LiPo. A pseudo-2-dimensional electrochemical model was coupled with a 3D thermal model using COMSOL Multiphysics® to determine the working voltage and temperature during discharge and was compared with experimental data from a commercial LiPo battery and evaluated using Root Mean Square Error (RMSE). The simulated discharge curve agrees remarkably well with the experimental results. The simulated temperature profile has shown appreciable discrepancies primarily due to the generated entropic change coefficient values that significantly affect the battery's heat generation. Overall, the models can be employed as a design tool to evaluate the component design and estimate the system performance of LiPo batteries for commercial applications. Furthermore, researchers can expand the study to investigate more advanced electrochemical phenomena and performances of state-of-the-art lithium and post-lithium chemistries.

## 1. Introduction

One of the most critical challenges facing the rising energy demand is developing a reliable energy storage system that will provide a long cycle and stable energy output without sacrificing safety. Lithium-ion batteries (LIBs) have been ubiquitous energy storage technologies for various electrical systems, from communication purposes to transportation applications (Gandolfo et al., 2015). LIB has been the prevailing technology in the market because of its high energy density, rechargeability, and portability. LIBs that commonly employ liquid-based electrolytes despite having good electrochemical properties suffer from safety and performance issues due to uncontrolled temperature build-up. Thus, cell manufacturers have doubled their efforts to substitute liquid electrolytes with more robust and safer alternatives such as solid and semisolids. LiPo batteries are a subcategory of LIBs that uses a solid or semisolid (gel) polymer (GPE) that can act as a separator and electrolyte for the system. LiPo batteries that use GPEs are increasing in interest because of their ability of non-leakage, flexibility, stability, lower resistance between electrode and electrolyte compared to solid electrolytes, and high ionic conductivity. Compared to a conventional liquid electrolyte, gel polymer electrolyte is more thermally and electrochemically stable, therefore, comparatively safer. Despite having an overall safer mechanism, LiPo batteries have lower general electrochemical performance and poor cyclability. Thus, studies of LiPo batteries give vital importance to enhancing their electrochemical performance, cycle life, reliability, and safety without compensating for marketable costs (Zhou et al., 2019).

The number of studies on LiPo battery material modification has been growing recently with various material compositions. Although various companies produce many different LiPo batteries, a relatively limited number of studies have been conducted concerning modeling and simulation. To assist with experimental approaches, it is necessary to develop fundamental insights into the battery's complex electrochemical, thermal, and mass transport mechanisms (Castro et al., 2021). Modeling and simulation of batteries are economical and powerful tools to provide the necessary framework of the battery's behavior at different operating conditions, evaluate the battery's performance, and analyze the material composition's effect on the useful lifecycle of the battery. Multiphysics modeling allows a solution to synergistic behaviors such as electrochemical and thermal by solving nonlinear partial differential equations using the finite element method. Because the model incorporates the battery electrochemical reactions and interactions, battery behavior at different conditions could be predicted with high accuracy and precision (le Houx and Kramer, 2020). Numerical methods alongside experimental methods are integral in developing a better design and better material composition for high-performance batteries. Despite LiPo batteries reaching commercialization, no study exists in multiphysics modeling of LCO-based LiPo batteries. This study developed a multiphysics model for a graphite/PVdF-HFP/LCO pouch-type commercial LiPo battery and compared electrochemical and thermal behavior results to experimental data.

## 2. Methodology

The methodology is divided into two parts, and schematics are shown in Figure 1. First is the experimental determination of the electrochemical-thermal behavior of the LiPo battery. The second is the multiphysics modeling of the battery using literature-based parameters. The model is then validated by comparing experimental and simulation results.

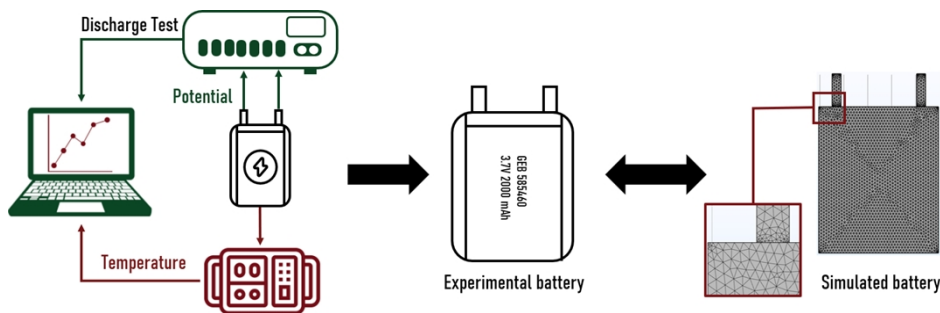


Figure 1: Schematic representation of methodology from experimental setup to simulating behavior using the generated electrochemical-thermal model.

### 2.1 Experimental setup

The experimental setup analyzes the electrochemical and thermal behavior of the commercial LiPo battery with specifications listed in Table 1 during 1C discharge rate (a current of 2 A) with a cut-off voltage of 3.1 V. The electrochemical analysis was done using an AUTOLAB PGSTAT302N potentiostat where the working voltage at ambient temperature was determined during discharge. Thermal behavior was conducted by analyzing the battery's surface temperature during discharge. The temperature was logged using a Hydra data logger with two thermocouples situated at the center of the battery cell on two sides each. The average temperature from the thermocouples designates the average battery surface temperature.

Table 1: LiPo battery specifications

Property	Value
Battery model	GEB 585460
Nominal capacity [mAh]	2,000
Nominal voltage [V]	3.7
Maximum charge voltage [V]	4.2
Charge current: Standard [A]	0.4
Maximum discharge current [A]	2
Discharge cut-off voltage [V]	2.75
Weight [g]	37.5
Dimensions (Length*Width*Thickness) [mm]	54.5 × 49.3 × 4.8

## 2.2 Multiphysics modeling

The multiphysics model uses the same geometry and chemistry as the experimental LiPo battery. The model uses a pseudo-2D (P2D) electrochemical model proposed by Doyle and Newman comprising of a one-dimensional geometry consisting of the two electrodes and their respective current collectors and the separator. The P2D model consists of Ohm's law to determine the current density by the solid phase charge transport, the concentrated solution theory for charge transport and mass transport in the electrolyte phase, and Fick's law for the mass transport in the solid phase. Tortuosity properties are provided by the Bruggeman correlation and were used to encompass the effect of porosity on mass and charge transport. Butler-Volmer kinetics described the relationship between the electrochemical reaction rate on concentration and current density (Doyle and Newman, 1995). The thermal model was based on the works of Bahiraei et al. (2017), which analyzed the thermal effects of a graphite/LiNiCoAlO<sub>2</sub> battery. The thermal properties were substituted in the literature model to tailor-fit the LiPo battery chemistry. The model was based on the energy balance produced and released by the battery referred to in Eq(1). The energy balance accounts for the accumulated heat, heat transfer by convection and conduction, and heat generation. The thermal model uses a 3D geometry consisting of the bulk active battery material properties. The battery heat generation acquired from the P2D electrochemical model is described in Eq(2), which comprises the reversible and irreversible heat generation designated by the first term and second term on the right-hand side of the equation. The irreversible heat generation consists of polarization and ohmic heat. Eq(2) was used to solve the battery heat generation,  $q_B$  which was substituted then to the energy balance equation, Eq(1), to solve for the average battery temperature,  $T$ .

$$\rho c_p \frac{\partial T}{\partial t} = \lambda \nabla^2 T + q_B \quad (1)$$

$$q_B = \left( ai_n T \frac{\partial U_{eq}}{\partial T} \right) + (q_{pol} + q_{ohm}) \quad (2)$$

The average temperature from the 3D thermal model was carried in the P2D electrochemical model. The average heat generation from the P2D model was added as a heat source to the 3D thermal model. The coupled multiphysics model determined the working voltage and average surface battery temperature during 1C discharge rate. The parameters used in the study are presented in Table 2. The model results were validated by computing the RMSE of the discharge curve and temperature profile in contrast with the experimental results.

Table 2: LiPo battery multiphysics model parameters

Parameter	Cathode CC	Cathode	Separator	Anode	Anode CC
Solid phase volume fraction	1	0.59 [a]		0.49 [a]	1
Electrolyte phase volume fraction	0	0.45	0.45	0.45	0
Initial Li <sup>+</sup> concentration in solid [mol/m <sup>3</sup> ]		21,250 [*]		23,099.58 [b]	
Max. Li <sup>+</sup> concentration in solid [mol/m <sup>3</sup> ]		51,554 [a]		30,555 [a]	
Electronic conductivity [S/m]	3.8×10 <sup>7</sup> [a]	10 [a]		100 [a]	6×10 <sup>7</sup> [a]
Transference number			0.435 [b]		
Ionic conductivity [m <sup>2</sup> /s]		from [a]	from [a]	from [a]	
Equilibrium potential [V]		from [a]		from [a]	
Entropic change coefficient [V/K]		from [a]		from [c]	
Thermal conductivity (W/mK)	238 [d]	1.48 [d]	0.45 [d]	1.04 [d]	398 [d]
Isobaric heat capacity [J/kgK]	903 [d]	700 [d]	133.9 [d]	1,437.4 [d]	385 [d]
Density [kg/m <sup>3</sup> ]	1,500 [d]	2,500 [d]	1,290 [d]	2,660 [d]	8,900 [d]

CC refers to the current collector. [\*] Fitted to experimental data. [a] (Zhang et al., 2020), [b] (Lamorgese et al., 2018), [c] (Rheinfeld et al., 2019), [d] (Peng et al., 2014), and parameters without designations were taken from (Cai and White, 2011).

## 3. Results and discussion

### 3.1 Electrochemical behavior

The cell's open circuit potential (OCP) is the difference between the negative and positive electrode potential and depends on the electrode materials. The OCP is a strong function of the electrode's state of charge (SOC). During discharge, the SOC of the cathode starts from a low SOC and rises as the discharge continues, while the SOC of the anode starts from a high value and drops upon discharge. This phenomenon demonstrates the

deintercalation of lithium ions from the anode to the cathode during discharge. Figure 2 shows the electrochemical behavior of the LiPo battery, where Figure 2a exhibits the OCP of the electrodes as SOC increases to unity, designating complete lithiation of the material. A good cathode material should have a high OCP that would define the higher cut-off voltage of the battery during charge. For an LCO cathode used in this study, the cut-off voltage was 4.2 V which is within the range of OCP in Figure 2a. Three transition regions exist for the LCO corresponding to changes in the metal structure due to lithiation. The ordering stages designate the order during discharge, where the cathode starts at a low SOC while the anode starts at high SOC. From a delithiated state at the start of discharge, the LCO changes from a monoclinic to hexagonal structure (stage I). Then, as lithiation proceeds, the hexagonal structure reverts to a monoclinic structure (stage II), and finally, a first-order two-phase region of rhombohedral structure defining the plateau region (stage III) (Mohamed and Allam, 2020). The graphite anode at stage I holds lithium ions in an ordered array in its hexagonal structure from a lithiated state at the start of discharge. As discharge proceeds, stage II lithium ions are inserted at every other graphene layer and finally at a delithiated state; stage III lithium ions are randomly distributed between layers returning to pure graphite at complete delithiation (Yazami and Reynier, 2006). For both electrodes, a plateau region can be seen for cathode SOC > 0.5 and anode SOC > 0.2. These plateau regions determine the battery's normal operating voltage, the difference between the electrodes' OCP of around 3.7 V.

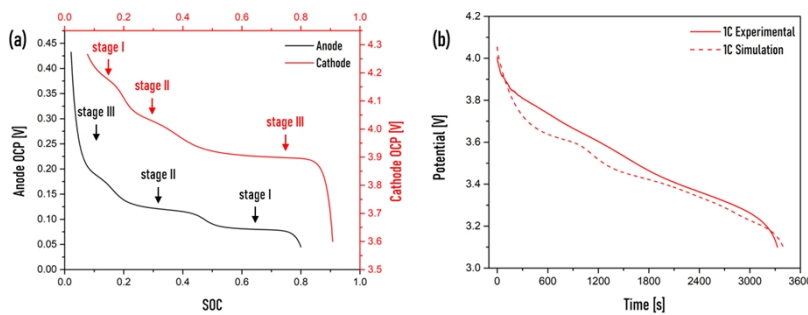


Figure 2: (a) Generated OCP curves for (red) cathode and (black) anode as a function of SOC, and (b) Comparison of (dashed line) experimental and (solid line) simulated 1C discharge curve.

Figure 2b shows the comparison between the experimental and simulated discharge curve at a 1C rate. The experimental discharge curve resembles the works of Lamorgese et al. (2018), which uses an LCO-graphite battery using liquid electrolyte, where an initial voltage drop is present due to activation losses and a stagnant decrease in potential followed by a sudden drop of potential due to mass transport common in lithium-ion battery chemistries. The calculated RMSE for the 1C rate is 0.06 V using a timestep of 1 s, which can be used as a reliable first approximation for battery behavior prediction. The computational time for the 1C rate was 1 hour as the simulation ran both the electrochemical and thermal models simultaneously. It can be seen in Figure 2b that the simulated results agree well with the experimental result, verifying the accuracy of the simulated P2D model. The discharge of the actual battery drops to the cut-off voltage earlier than the simulated model. The discrepancy may be due to manufacturing band estimations as the actual capacity may not be exactly 2,000 mAh. In the simulated discharge curve, an abrupt slope difference can be seen at a time of 1,000 s, which was not profound in the experimental results. This sudden change in curvature indicates a two-step discharge profile grounded on the battery cell chemistry. For both simulation and experimental results, a slight plateau region can be recognized through the course of operation. A higher C rate is expected to decrease the discharge time and shorten the plateau region. This is primarily due to higher polarization at the higher discharge C rate, which leads to greater polarization heat generation, further propagating to higher battery temperature operation. Aside from the synergism of SOC and OCP, the simulated model's integrity may be heightened by incorporating additional parameters not focused on in this study, such as the active material volume fraction and porosity of the electrodes and measuring the actual solid-phase diffusion coefficients of the lithium-ion.

### 3.2 Thermal behavior

The battery's temperature is heavily dependent on the heat generation due to the electrochemical reactions taking place in the active battery material. The reversible and irreversible heat generation plays an influential role in the heat transfer of the battery. The reversible heat generation may either be endothermic or exothermic in nature, while the irreversible heat generation is always exothermic (Viswanathan et al., 2010). The entropic change coefficient of the electrodes dictates the reversible heat generation. It would depend on the material employed and the electrodes' SOC directly associated with the degree of lithiation. The entropy change

coefficient as a function of SOC can be seen in Figure 3a for both electrodes, where both cases exhibit either exothermic or endothermic entropic value depending on the degree of lithiation corresponding to the SOC. Figure 3b compares the average battery surface temperature during 1C discharge rate of the experimental and simulated runs. The experimental and simulated average battery surface temperature starts at about 303.5 K. The end of discharge reaches a maximum temperature of 311 K, corresponding to nearly a 7.5 K increase. Despite similar initial and final temperatures, the qualitative appearance of the temperature profile does not agree well, resulting in an RMSE value of 1.5153 K. The discrepancies may be accounted for by an array of factors. One source of error is the generated model assumes a homogenous heat generation in the active battery material. Another factor is that the entropic change coefficient used in the study was based on literature rather than actual experiments. The entropic change coefficient as a function of SOC for LCO dates back to the 1990s, and several studies have used this equation with numerical curve fittings to match their results which was no longer accounted for in this study (Egorkina and Skundin, 1998). Compared to modern experimental results analyzing LCO entropic change, exothermic heat release occurs for all SOC from 0 to 0.8, which is not analogous to the generated curve as an endothermic region (labeled as point A in Figure 3a) exists (Choudhari et al., 2020) This would entail that modern commercial batteries require rigorous experimental determination of critical electrochemical and thermal parameters to secure the numerical model's reliability and accuracy.

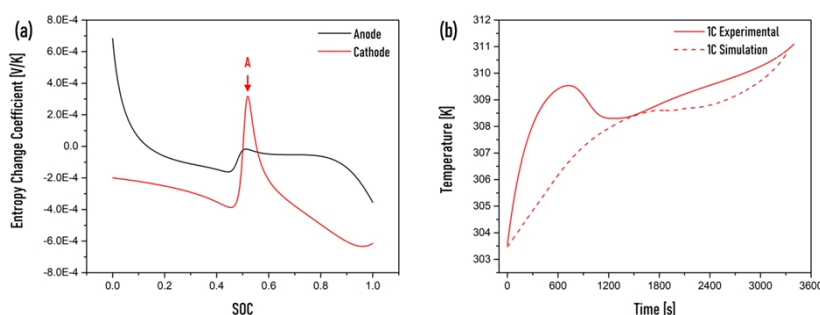


Figure 3: (a) Generated entropy change coefficient for (red) cathode and (black) anode as a function of SOC, and (b) Comparison of (dashed line) experimental and (solid line) simulated thermal profile at 1C discharge rate.

During discharge, the temperature profile presents three stages for both simulation and experiment: the initial temperature rise, temperature drop (for the simulation) or buffering region (experimental), and final temperature rise. As the irreversible heat generation always releases heat, the initial temperature rise is due to the exothermic heat release of the reversible and irreversible heat. The model uses an initial SOC of 0.4 for the cathode and 0.76 for the anode, where both these regions exhibit a negative entropy change coefficient expressing exothermic heat release. As the discharge operation proceeds, the anode SOC decreases, and the cathode SOC increases where the cathode observes a positive entropic region (where the peak region is labeled as A) where the material absorbs heat from the surrounding, and in turn, the battery temperature drops or hinders its increase. Despite the anode experiencing exothermic behavior, the cathode endothermic entropy out measures the anode contribution. Furthermore, as the temperature of the battery increases, the temperature gradient between the battery and surrounding increases leading to an increase in heat dissipation due to convection preventing the temperature rise. The last phase is the final temperature rise. It can be observed in Figure 3a that an endothermic region exists for the anode at SOC below 0.13; however, the cathode releases exothermic heat at high SOC and the inherent exothermic irreversible heat generation. Irreversible heat is expected to rise at the end of discharge due to an increase in overpotential. This combined effect of the entropy of the cathode and increased irreversible heat overweighs the endothermic entropy of the anode, increasing the battery temperature during the final phase of discharge.

#### 4. Conclusions

A multiphysics model was successfully developed for a graphite/ PVdF-HFP/ LCO pouch LiPo battery capturing the electrochemical-thermal behavior using COMSOL Multiphysics®. The simulated model consisted of a P2D electrochemical and 3D thermal models and was compared using experimental results using a commercial GEB 585460 LiPo battery. Simulated electrochemical behavior by determining the discharge curve at a 1C rate was investigated and validated, showing competitive accuracy. Simulation results show a two-step discharge phenomenon for the battery but were not profound in the experimental cell. Simulated thermal behavior during discharge showed appreciable discrepancies from experimental results. The simulated thermal profile showed a prominent decrease in average surface battery temperature, absent in the experiment. The temperature

lowering by heat absorption was primarily due to the reversible heat generation where endothermic values were present in the simulation. As the electrochemical and thermal models were coupled by the temperature and heat generation, both models' veracity heavily relies on the accuracy of parameters determined in the literature used by the study. The generated model can be extended to analyze thermal runaway behavior of the battery as well as developing a sensitivity analysis toward the model parameters. Overall, the developed multiphysics model can serve as an initial bird's-eye view in predicting battery behavior at various operational conditions.

### Nomenclature

$c_p$ – isobaric specific heat, J/(kg·K)	$q_{ohm}$ – ohmic heat generation, W/m <sup>3</sup>
$i_n$ – local current density, A/m <sup>2</sup>	$q_{pol}$ – polarization heat generation, W/m <sup>3</sup>
$T$ – local temperature, K	$\alpha$ – specific surface area, 1/m
$t$ – time, s	$\lambda$ – thermal conductivity, W/(m·K)
$U_{eq}$ – equilibrium potential, V	$\rho$ – density, kg/m <sup>3</sup>
$q_B$ – battery heat generation, W/m <sup>3</sup>	$\eta$ – overpotential, V

### Acknowledgments

M.R.B.D. would like to acknowledge the Engineering Research and Development for Technology (ERDT) Graduate Scholarship. J.A.D.D. would like to acknowledge the Center for Advanced Batteries Program funded by the Department of Science and Technology (DOST) through the Niche Centers in the Regions for R&D (NICER) Program.

### References

- Bahiraee, F., Ghalkhani, M., Fartaj, A., Nazri, G. A., 2017, A pseudo 3D electrochemical-thermal modeling and analysis of a lithium-ion battery for electric vehicle thermal management applications. *Applied Thermal Engineering*, 125, 904–918.
- Cai, L., White, R. E., 2011, Mathematical modeling of a lithium ion battery with thermal effects in COMSOL Inc. Multiphysics (MP) software. *Journal of Power Sources*, 196(14), 5985–5989.
- Castro, M. T., del Rosario, J. A. D., Chong, M. N., Chuang, P.-Y. A., Lee, J., Ocon, J. D., 2021, Multiphysics modeling of lithium-ion, lead-acid, and vanadium redox flow batteries. *Journal of Energy Storage*, 42, 102982.
- Choudhari, V. G., Dhoble, D. A. S., Sathe, T. M., 2020, A review on effect of heat generation and various thermal management systems for lithium ion battery used for electric vehicle. *Journal of Energy Storage*, 32, 101729.
- Doyle, M., Newman, J., 1995, The use of mathematical modeling in the design of lithium/polymer battery systems. *Electrochimica Acta*, 40(13–14), 2191–2196.
- Egorkina, O. Y., Skundin, A. M., 1998, The effect of temperature on lithium intercalation into carbon materials. *Journal of Solid State Electrochemistry* 1998 2:4, 2(4), 216–220.
- Gandolfo, D., Brandão, A., Patiño, D., Molina, M., 2015, Dynamic model of lithium polymer battery – Load resistor method for electric parameters identification. *Journal of the Energy Institute*, 88(4), 470–479.
- Lamorgese, A., Mauri, R., Tellini, B., 2018, Electrochemical-thermal P2D aging model of a LiCoO<sub>2</sub>/graphite cell: Capacity fade simulations. *Journal of Energy Storage*, 20, 289–297.
- le Houx, J., Kramer, D., 2020, Physics based modelling of porous lithium ion battery electrodes—A review. *Energy Reports*, 6, 1–9.
- Mohamed, N., Allam, N. K., 2020, Recent advances in the design of cathode materials for Li-ion batteries. *RSC Advances*, 10(37), 21662–21685.
- Peng, P., Sun, Y., Jiang, F., 2014, Thermal analyses of LiCoO<sub>2</sub> lithium-ion battery during oven tests. *Heat and Mass Transfer*, 50(10), 1405–1416.
- Rheinfeld, A., Sturm, J., Noel, A., Wilhelm, J., Kriston, A., Pfrang, A., Jossen, A., 2019, Quasi-Isothermal External Short Circuit Tests Applied to Lithium-Ion Cells: Part II. Modeling and Simulation. *Journal of The Electrochemical Society*, 166(2), A151–A177.
- Viswanathan, V. v., Choi, D., Wang, D., Xu, W., Towne, S., Williford, R. E., Zhang, J. G., Liu, J., Yang, Z., 2010, Effect of entropy change of lithium intercalation in cathodes and anodes on Li-ion battery thermal management. *Journal of Power Sources*, 195(11), 3720–3729.
- Yazami, R., Reynier, Y., 2006, Thermodynamics and crystal structure anomalies in lithium-intercalated graphite. *Journal of Power Sources*, 153(2), 312–318.
- Zhang, L., Zhao, P., Xu, M., Wang, X., 2020, Computational identification of the safety regime of Li-ion battery thermal runaway. *Applied Energy*, 261, 114440.
- Zhou, D., Shanmukaraj, D., Tkacheva, A., Armand, M., Wang, G., 2019, Polymer Electrolytes for Lithium-Based Batteries: Advances and Prospects. *Chem*, 5(9), 2326–2352.